DENOISING DIFFUSION BRIDGE MODELS

Linqi Zhou **Aaron Lou** **Samar Khanna** **Stefano Ermon**
Department of Computer Science, Stanford University
{linqizhou, aaronlou, samar.khanna, ermon}@stanford.edu

ABSTRACT

Diffusion models are powerful generative models that map noise to data using stochastic processes. However, for many applications such as image editing, the model input comes from a distribution that is not random noise. As such, diffusion models must rely on cumbersome methods like guidance or projected sampling to incorporate this information in the generative process. In our work, we propose Denoising Diffusion Bridge Models (DDBMs), a natural alternative to this paradigm based on *diffusion bridges*, a family of processes that interpolate between two paired distributions given as endpoints. Our method learns the score of the diffusion bridge from data and maps from one endpoint distribution to the other by solving a (stochastic) differential equation based on the learned score. Our method naturally unifies several classes of generative models, such as score-based diffusion models and OT-Flow-Matching, allowing us to adapt existing design and architectural choices to our more general problem. Empirically, we apply DDBMs to challenging image datasets in both pixel and latent space. On standard image translation problems, DDBMs achieve significant improvement over baseline methods, and, when we reduce the problem to image generation by setting the source distribution to random noise, DDBMs achieve comparable FID scores to state-of-the-art methods despite being built for a more general task.

1 INTRODUCTION

Diffusion models are a powerful class of generative models which learn to reverse a diffusion process mapping data to noise (Sohl-Dickstein et al., 2015; Song and Ermon, 2019; Ho et al., 2020; Song et al., 2020b). For image generation tasks, they have surpassed GAN-based methods (Goodfellow et al., 2014) and achieved a new state-of-the-art for perceptual quality (Dhariwal and Nichol, 2021). Furthermore, these capabilities have spurred the development of modern text-to-image generative AI systems(Ramesh et al., 2022).

Despite these impressive results, standard diffusion models are ill-suited for other tasks. In particular, the diffusion framework assumes that the prior distribution is random noise, which makes it difficult to adapt to tasks such as image translation, where the goal is to map between pairs of images. As such, one resorts to cumbersome techniques, such as conditioning the model (Ho and Salimans, 2022; Saharia et al., 2021) or manually altering the sampling procedure (Meng et al., 2022; Song et al., 2020b). These methods are not theoretically principled and map in one direction (typically from corrupted to clean images), losing the cycle consistency condition (Zhu et al., 2017).

Instead, we consider methods which directly model a transport between two arbitrary probability distributions. This framework naturally captures the desiderata of image translation, but existing methods fall short empirically. For instance, ODE based flow-matching methods (Lipman et al., 2023; Albergo and Vanden-Eijnden, 2023; Liu et al., 2022a), which learn a deterministic path between two arbitrary probability distributions, have mainly been applied to image generation problems and have not been investigated for image translation. Furthermore, on image generation, ODE methods have not achieved the same empirical success as diffusion models. Schrödinger Bridge and models (De Bortoli et al., 2021) are another type of model which instead learn an entropic optimal transport between two probability distributions. However, these rely on expensive iterative approximation methods and have also found limited empirical use. More recent extensions including Diffusion Bridge Matching (Shi et al., 2023; Peluchetti, 2023) similarly require expensive iterative calculations.

In our work, we seek a scalable alternative that unifies diffusion-based unconditional generation methods and transport-based distribution translation methods, and we name our general framework Denoising Diffusion Bridge Models (DDBMs). We consider a reverse-time perspective of *diffusion bridges*, a diffusion process conditioned on given endpoints, and use this perspective to establish a general framework for distribution translation. We then note that this framework subsumes existing generative modeling paradigms such as score matching diffusion models (Song et al., 2020b) and flow matching optimal transport paths (Albergo and Vanden-Eijnden, 2023; Lipman et al., 2023; Liu et al., 2022a). This allows us to reapply many design choices to our more general task. In particular, we use this to generalize and improve the architecture pre-conditioning, noise schedule, and model sampler, minimizing input sensitivity and stabilizing performance. We then apply DDBMs to high-dimensional images using both pixel and latent space based models. For standard image translation tasks, we achieve better image quality (as measured by FID (Heusel et al., 2017)) and significantly better translation faithfulness (as measured by LPIPS (Zhang et al., 2018) and MSE). Furthermore, when we reduce our problem to image generation, we match standard diffusion model performance.

2 Preliminaries

Recent advances in generative models have relied on the classical notion of transporting a data distribution $q_{\text{data}}(\mathbf{x})$ gradually to a prior distribution $p_{\text{prior}}(\mathbf{x})$ (Villani, 2008). By learning to reverse this process, one can sample from the prior and generate realistic samples.

2.1 Generative Modeling with Diffusion Models

Diffusion process. We are interested in modeling the distribution $q_{\text{data}}(\mathbf{x})$, for $\mathbf{x} \in \mathbb{R}^d$. We do this by constructing a diffusion process, which is represented by a set of time-indexed variables $\{\mathbf{x}_t\}_{t=0}^T$ such that $\mathbf{x}_0 \sim p_0(\mathbf{x}) := q_{\text{data}}(\mathbf{x})$ and $\mathbf{x}_T \sim p_T(\mathbf{x}) := p_{\text{prior}}(\mathbf{x})$. Here $q_{\text{data}}(\mathbf{x})$ is the initial "data" distribution and $p_{\text{prior}}(\mathbf{x})$ is the final "prior" distribution. The process can be modeled as the solution to the following SDE

$$d\mathbf{x}_t = \mathbf{f}(\mathbf{x}_t, t)dt + g(t)d\mathbf{w}_t \tag{1}$$

where $\mathbf{f} : \mathbb{R}^d \times [0, T] \to \mathbb{R}^d$ is vector-valued *drift* function, $g : [0, T] \to \mathbb{R}$ is a scalar-valued *diffusion* coefficient, and $\mathbf{w}_t$ is a Wiener process. Following this diffusion process forward in time constrains the final variable $\mathbf{x}_T$ to follow distribution $p_{\text{prior}}(\mathbf{x})$. The reverse of this process is given by

$$d\mathbf{x}_t = \mathbf{f}(\mathbf{x}_t, t) - g(t)^2 \nabla_{\mathbf{x}_t} \log p(\mathbf{x}_t))dt + g(t)d\mathbf{w}_t \tag{2}$$

where $p(\mathbf{x}_t) := p(\mathbf{x}_t, t)$ is the marginal distribution of $\mathbf{x}_t$ at time t. Furthermore, one can derive an equivalent deterministic process called the probability flow ODE (Song et al., 2020b), which has the same marginal distributions:

$$d\mathbf{x}_t = \left[\mathbf{f}(\mathbf{x}_t, t) - \frac{1}{2} g(t)^2 \nabla_{\mathbf{x}_t} \log p(\mathbf{x}_t)\right] dt \tag{3}$$

In particular, one can draw $\mathbf{x}_T \sim q_{\text{data}}(\mathbf{y})$ and sample q_{data} by solving either the above reverse SDE or ODE backward in time.

Denoising score-matching. The score, $\nabla_{\mathbf{x}_t} \log p(\mathbf{x}_t)$, can be learned by the score-matching loss

$$\mathcal{L}(\theta) = \mathbb{E}_{\mathbf{x}_t \sim p(\mathbf{x}_t|\mathbf{x}_0), \mathbf{x}_0 \sim q_{\text{data}}(\mathbf{x}), t \sim \mathcal{U}(0,T)} \left[\|\mathbf{s}_\theta(\mathbf{x}_t, t) - \nabla_{\mathbf{x}_t} \log p(\mathbf{x}_t \mid \mathbf{x}_0)\|^2 \right] \tag{4}$$

such that the minimizer $\mathbf{s}_\theta^*(\mathbf{x}_t, t)$ of the above loss approximates the true score. Crucially, the above loss is tractable because the transition kernel $p(\mathbf{x}_t \mid \mathbf{x}_0)$, which depends on specific choices of drift and diffusion functions, is designed to be Gaussian $\mathbf{x}_t = \alpha_t \mathbf{x}_0 + \sigma_t \boldsymbol{\epsilon}$, where α_t and σ_t are functions of time and $\boldsymbol{\epsilon} \sim \mathcal{N}(\mathbf{0}, \boldsymbol{I})$. It is also common to view the diffusion process in terms of the $\mathbf{x}_t$'s signal-to-noise ratio (SNR), defined as α_t^2/σ_t^2.

2.2 Diffusion Process with Fixed Endpoints

Diffusion models are limited because they can only transport complex data distributions to a standard Gaussian distribution and cannot be naturally adapted to translating between two arbitrary distributions, *e.g.* in the case of image-to-image translation. Luckily, classical results have shown that one can condition a diffusion process on a fixed known endpoint via the famous Doob's h-transform:

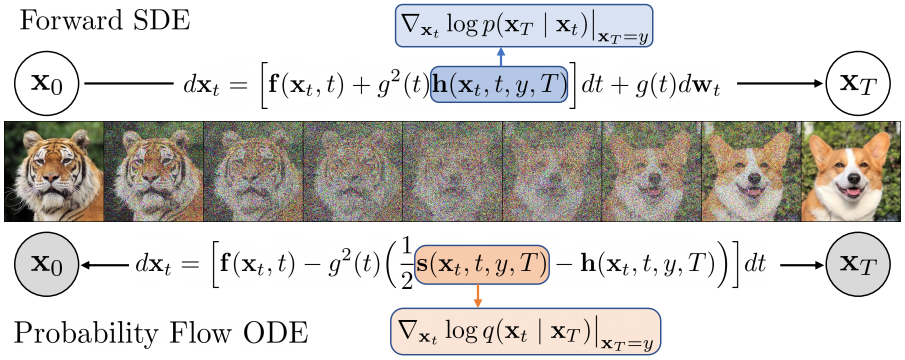

Figure 1: **A schematic for Denoising Diffusion Bridge Models.** DDBM uses a diffusion process guided by a drift adjustment (in blue) towards an endpoint $\mathbf{x}_T = y$. They lears to reverse such a bridge process by matching the denoising bridge score (in orange), which allows one to reverse from $\mathbf{x}_T$ to $\mathbf{x}_0$ for any $\mathbf{x}_T = \mathbf{y} \sim q_{\text{data}}(\mathbf{y})$. The forward SDE process shown on the top is unidirectional while the probability flow ODE shown at the bottom is deterministic and bidirectional. White nodes are stochastic while grey nodes are deterministic.

Stochastic bridges via h-transform. Specifically, a diffusion process defined in Eq. (1) can be driven to arrive at a particular point of interest $y \in \mathbb{R}^d$ almost surely via Doob's h-transform (Doob and Doob, 1984; Rogers and Williams, 2000),

$$d\mathbf{x}_t = \mathbf{f}(\mathbf{x}_t, t)dt + g(t)^2\mathbf{h}(\mathbf{x}_t, t, y, T) + g(t)d\mathbf{w}_t, \quad \mathbf{x}_0 \sim q_{\text{data}}(\mathbf{x}), \quad \mathbf{x}_T = y \tag{5}$$

where $\mathbf{h}(x, t, y, T) = \nabla_{\mathbf{x}_t} \log p(\mathbf{x}_T \mid \mathbf{x}_t)\big|_{\mathbf{x}_t=x, \mathbf{x}_T=y}$ is the gradient of the log transition kernel of from t to T generated by the original SDE, evaluated at points $\mathbf{x}_t = x$ and $\mathbf{x}_T = y$, and each $\mathbf{x}_t$ now explicitly depends on y at time T. Furthermore, $p(\mathbf{x}_T = y \mid \mathbf{x}_t)$ satisfies the Kolmogorov backward equation (specified in Appendix A). With specific drift and diffusion choices, *e.g.* $\mathbf{f}(\mathbf{x}_t, t) = \mathbf{0}$, $\mathbf{h}$ is tractable due to the tractable (Gaussian) transition kernel of the underlying diffusion process.

When the initial point $\mathbf{x}_0$ is fixed, the process is often called a *diffusion bridge* (Särkkä and Solin, 2019; Heng et al., 2021; Delyon and Hu, 2006; Schauer et al., 2017; Peluchetti; Liu et al., 2022b), and its ability to connect any given $\mathbf{x}_0$ to a given value of $\mathbf{x}_T$ is promising for image-to-image translation. Furthermore, the transition kernel may be tractable, which serves as further motivation.

3 Denoising Diffusion Bridge Models

Assuming that the endpoints of a diffusion bridge both exist in $\mathbb{R}^d$ and come from an arbitrary and unknown joint distribution, *i.e.* $(\mathbf{x}_0, \mathbf{x}_T) = (\mathbf{x}, \mathbf{y}) \sim q_{\text{data}}(\mathbf{x}, \mathbf{y})$, we wish to devise a process that learns to approximately sample from $q_{\text{data}}(\mathbf{x} \mid \mathbf{y})$ by reversing the diffusion bridge with boundary distribution $q_{\text{data}}(\mathbf{x}, \mathbf{y})$, given a training set of *paired* samples drawn from $q_{\text{data}}(\mathbf{x}, \mathbf{y})$.

3.1 Time-Reversed SDE and Probability Flow ODE

Inspired by diffusion bridges, we construct the stochastic process $\{\mathbf{x}_t\}_{t=0}^T$ with marginal distribution $q(\mathbf{x}_t)$ such that $q(\mathbf{x}_0, \mathbf{x}_T)$ approximates $q_{\text{data}}(\mathbf{x}_0, \mathbf{x}_T)$. Reversing the process amounts to sampling from $q(\mathbf{x}_t \mid \mathbf{x}_T)$. Note that distribution $q(\cdot)$ is different from $p(\cdot)$, *i.e.* the diffusion marginal distribution, in that the endpoint distributions are now $q_{\text{data}}(\mathbf{x}_0, \mathbf{x}_T) = q_{\text{data}}(\mathbf{x}, \mathbf{y})$ instead of the distribution of a diffusion $p(\mathbf{x}_0, \mathbf{x}_T) = p(\mathbf{x}_T \mid \mathbf{x}_0)q_{\text{data}}(\mathbf{x}_0)$, which defines a Gaussian $\mathbf{x}_T$ given $\mathbf{x}_0$. We can construct the time-reversed SDE/probability flow ODE of $q(\mathbf{x}_t \mid \mathbf{x}_T)$ via the following theorem.

Theorem 1. *The evolution of conditional probability $q(\mathbf{x}_t \mid \mathbf{x}_T)$ has a time-reversed SDE of the form*

$$d\mathbf{x}_t = \Big[\mathbf{f}(\mathbf{x}_t, t) - g^2(t)\Big(\mathbf{s}(\mathbf{x}_t, t, y, T) - \mathbf{h}(\mathbf{x}_t, t, y, T)\Big)\Big]dt + g(t)d\hat{\mathbf{w}}_t, \quad \mathbf{x}_T = y \tag{6}$$

with an associated probability flow ODE

$$d\mathbf{x}_t = \Big[\mathbf{f}(\mathbf{x}_t, t) - g^2(t)\Big(\frac{1}{2}\mathbf{s}(\mathbf{x}_t, t, y, T) - \mathbf{h}(\mathbf{x}_t, t, y, T)\Big)\Big]dt, \quad \mathbf{x}_T = y \tag{7}$$

Figure 2: VE bridge (left) and VP bridge (right) with their SDE (top) and ODE (bottom) visualization.

	$\mathbf{f}(\mathbf{x}_t, t)$	$g^2(t)$	$p(\mathbf{x}_t \mid \mathbf{x}_0)$	SNR_t	$\nabla_{\mathbf{x}_t} \log p(\mathbf{x}_T \mid \mathbf{x}_t)$
VP	$\frac{d \log \alpha_t}{dt}\mathbf{x}_t$	$\frac{d}{dt}\sigma_t^2 - 2\frac{d \log \alpha_t}{dt}\sigma_t^2$	$\mathcal{N}(\alpha_t \mathbf{x}_0, \sigma_t^2 \boldsymbol{I})$	α_t^2/σ_t^2	$\frac{(\alpha_t/\alpha_T)\mathbf{x}_T - \mathbf{x}_t}{\sigma_t^2(\text{SNR}_t/\text{SNR}_T - 1)}$
VE	$\mathbf{0}$	$\frac{d}{dt}\sigma_t^2$	$\mathcal{N}(\mathbf{x}_0, \sigma_t^2 \boldsymbol{I})$	$1/\sigma_t^2$	$\frac{\mathbf{x}_T - \mathbf{x}_t}{\sigma_T^2 - \sigma_t^2}$

Table 1: VP and VE instantiations of diffusion bridges.

on $t \leq T - \epsilon$ for any $\epsilon > 0$, where $\hat{\mathbf{w}}_t$ denotes a Wiener process, $\mathbf{s}(x, t, y, T) = \nabla_{\mathbf{x}_t} \log q(\mathbf{x}_t \mid \mathbf{x}_T)\big|_{\mathbf{x}_t = x, \mathbf{x}_T = y}$ and $\mathbf{h}$ is as defined in Eq. (5).

A schematic of the bridge process is shown in Figure 1. Note that this process is defined up to $T - \epsilon$. To recover the initial distribution in the SDE case, we make an approximation that $\mathbf{x}_{T-\epsilon} \approx y$ for some small ϵ simulate SDE backward in time. For the ODE case, since we need to sample from $p(\mathbf{x}_{T-\epsilon})$ which cannot be Dirac delta, we cannot approximate $\mathbf{x}_{T-\epsilon}$ with a single y. Instead, we can first approximate $\mathbf{x}_{T-\epsilon'} \approx y$ where $\epsilon > \epsilon' > 0$, and then take an Euler-Maruyama step to $\mathbf{x}_{T-\epsilon}$, and Eq. (7) can be used afterward. A toy visualization of VE bridge and VP bridges are shown in Figure 2. The top and bottom shows the respective SDE and ODE paths for VE and VP bridges.

3.2 Marginal Distributions and Denoising Bridge Score Matching

The sampling process in Theorem 1 requires approximation of the score $\mathbf{s}(x, t, y, T) = \nabla_{\mathbf{x}_t} \log q(\mathbf{x}_t \mid \mathbf{x}_T)\big|_{\mathbf{x}_t = x, \mathbf{x}_T = y}$ where $q(\mathbf{x}_t \mid \mathbf{x}_T) = \int_{\mathbf{x}_0} q(\mathbf{x}_t \mid \mathbf{x}_0, \mathbf{x}_T) q_{\text{data}}(\mathbf{x}_0 \mid \mathbf{x}_T) d\mathbf{x}_0$. However, as the true score is not known in closed-form, we take inspiration from denoising score-matching (Song et al., 2020b) and use a neural network to approximate the true score by matching against a tractable quantity. This usually results in closed-form marginal sampling of $\mathbf{x}_t$ given data (*e.g.* $\mathbf{x}_0$ in the case of diffusion models and $(\mathbf{x}_0, \mathbf{x}_T)$ in our case), and given $\mathbf{x}_t$, the model is trained to match against the closed-form denoising score objective. We are motivated to follow a similar approach because (1) tractable marginal sampling of $\mathbf{x}_t$ and (2) closed-form objectives enable a simple and scalable algorithm. We specify how to design the marginal sampling distribution and the tractable score objective below to approximate the ground-truth conditional score $\nabla_{\mathbf{x}_t} \log q(\mathbf{x}_t \mid \mathbf{x}_T)$.

Sampling distribution. Fortunately, for the former condition, we can design our sampling distribution $q(\cdot)$ such that $q(\mathbf{x}_t \mid \mathbf{x}_0, \mathbf{x}_T) := p(\mathbf{x}_t \mid \mathbf{x}_0, \mathbf{x}_T)$, where $p(\cdot)$ is the diffusion distribution pinned at both endpoints as in Eq. (5). For diffusion processes with Gaussian transition kernels, *e.g.* VE, VP (Song et al., 2020b), our sampling distribution is a Gaussian distribution of the form

$$
\begin{aligned}
q(\mathbf{x}_t \mid \mathbf{x}_0, \mathbf{x}_T) &= \mathcal{N}(\hat{\mu}_t, \hat{\sigma}_t^2 \boldsymbol{I}), \quad \text{where} \\
\hat{\mu}_t &= \frac{\text{SNR}_T}{\text{SNR}_t} \frac{\alpha_t}{\alpha_T} \mathbf{x}_T + \alpha_t \mathbf{x}_0 (1 - \frac{\text{SNR}_T}{\text{SNR}_t}) \\
\hat{\sigma}_t^2 &= \sigma_t^2 (1 - \frac{\text{SNR}_T}{\text{SNR}_t})
\end{aligned}
\tag{8}
$$

where α_t and σ_t are pre-defined signal and noise schedules and $\text{SNR}_t = \alpha_t^2/\sigma_t^2$ is the signal-to-noise ratio at time t. For VE schedule, we assume $\alpha_t = 1$ and derivation details are provided in Appendix A.1. Notably, the mean of this distribution is a linear interpolation between the (scaled) endpoints, and the distribution approaches a Dirac distribution when nearing either end. For concreteness, we present the bridge processes generated by both VP and VE diffusion in Table 1 and recommend choosing $\mathbf{f}$ and g specified therein.

Training objective. For the latter condition, diffusion bridges benefit from a similar setup as in diffusion models, since a pre-defined signal/noise schedule gives rise to a closed-form conditional score $\nabla_{\mathbf{x}_t} \log q(\mathbf{x}_t \mid \mathbf{x}_0, \mathbf{x}_T)$. We show in the following theorem that with $\mathbf{x}_t \sim q(\mathbf{x}_t \mid \mathbf{x}_0, \mathbf{x}_T)$, a neural network $\mathbf{s}_\theta(\mathbf{x}_t, \mathbf{x}_T, t)$ that matches against this closed-form score approximates the true score.

Theorem 2 (Denoising Bridge Score Matching)**.** *Let* $(\mathbf{x}_0, \mathbf{x}_T) \sim q_{\text{data}}(\mathbf{x}, \mathbf{y})$*,* $\mathbf{x}_t \sim q(\mathbf{x}_t \mid \mathbf{x}_0, \mathbf{x}_T)$*,* $t \sim p(t)$ *for any non-zero time sampling distribution* $p(t)$ *in* $[0, T]$*, and* $w(t)$ *be a non-zero loss weighting term of any choice. Minimum of the following objective:*

$$\mathcal{L}(\theta) = \mathbb{E}_{\mathbf{x}_t, \mathbf{x}_0, \mathbf{x}_T, t}\Big[w(t)\|\mathbf{s}_\theta(\mathbf{x}_t, \mathbf{x}_T, t) - \nabla_{\mathbf{x}_t} \log q(\mathbf{x}_t \mid \mathbf{x}_0, \mathbf{x}_T)\|^2\Big] \tag{9}$$

satisfies $\mathbf{s}_\theta(\mathbf{x}_t, \mathbf{x}_T, t) = \nabla_{\mathbf{x}_t} \log q(\mathbf{x}_t \mid \mathbf{x}_T)$.

In short, we establish a tractable diffusion bridge over two endpoints and, by matching the conditional score of the Gaussian bridge, we can learn the score of the new distribution $q(\mathbf{x}_t \mid \mathbf{x}_T)$ that satisfies the boundary distribution $q_{\text{data}}(\mathbf{x}, \mathbf{y})$.

4 Generalized Parameterization for Distribution Translation

Building the bridge process upon diffusion process allows us to further adapt many recent advancements in the score network parameterization $\mathbf{s}_\theta(\mathbf{x}_t, \mathbf{x}_T, t)$ (Ho et al., 2020; Song et al., 2020b; Salimans and Ho, 2022; Ho et al., 2022; Karras et al., 2022), different noise schedules, and efficient ODE sampling (Song et al., 2020a; Karras et al., 2022; Lu et al., 2022a;b; Zhang and Chen, 2022) to our more general framework. Among these works, EDM (Karras et al., 2022) proposes to parameterize the model output to be $D_\theta(\mathbf{x}_t, t) = c_{\text{skip}}(t)\mathbf{x}_t + c_{\text{out}}(t)F_\theta(c_{\text{in}}(t)\mathbf{x}_t, c_{\text{noise}}(t))$ where F_θ is a neural network with parameter θ that predicts $\mathbf{x}_0$. In a similar spirit, we adopt this pred-$\mathbf{x}$ parameterization and additionally derive a set of scaling functions for distribution translation, which we show is a strict superset.

Score reparameterization. Following the sampling distribution proposed in (8), a pred-$\mathbf{x}$ model can predict bridge score by

$$\nabla_{\mathbf{x}_t} \log q(\mathbf{x}_t \mid \mathbf{x}_T) \approx -\frac{\mathbf{x}_t - \Big(\frac{\text{SNR}_T}{\text{SNR}_t}\frac{\alpha_t}{\alpha_T}\mathbf{x}_T + \alpha_t D_\theta(\mathbf{x}_t, \mathbf{x}_T, t)(1 - \frac{\text{SNR}_T}{\text{SNR}_t})\Big)}{\sigma_t^2(1 - \frac{\text{SNR}_T}{\text{SNR}_t})} \tag{10}$$

Scaling functions and loss weighting. Following Karras et al. (2022), and let $a_t = \alpha_t/\alpha_T * \text{SNR}_T/\text{SNR}_t$, $b_t = \alpha_t(1 - \text{SNR}_T/\text{SNR}_t)$, $c_t = \sigma_t^2(1 - \text{SNR}_T/\text{SNR}_t)$, the scaling functions and weighting function $w(t)$ can be derived to be

$$c_{\text{in}}(t) = \frac{1}{\sqrt{a_t^2\sigma_T^2 + b_t^2\sigma_0^2 + 2a_t b_t \sigma_{0T} + c_t)}}, \quad c_{\text{out}}(t) = \sqrt{a_t^2(\sigma_T^2\sigma_0^2 - \sigma_{0T}^2) + \sigma_0^2 c_t} * c_{\text{in}}(t) \tag{11}$$

$$c_{\text{skip}}(t) = \Big(b_t\sigma_0^2 + a_t\sigma_{0T}\Big) * c_{\text{in}}^2(t), \quad w(t) = \frac{1}{c_{\text{out}}(t)^2}, \quad c_{\text{noise}}(t) = \frac{1}{4}\log(t) \tag{12}$$

where σ_0^2, σ_T^2, and σ_{0T} denote the variance of $\mathbf{x}_0$, variance of $\mathbf{x}_T$, and the covariance of the two, respectively. The only additional hyperparameters compared to EDM are σ_T and σ_{0T}, which characterize the distribution of $\mathbf{x}_T$ and its correlation with $\mathbf{x}_0$. One can notice that in the case of EDM, $\sigma_t = t$, $\sigma_T^2 = \sigma_0^2 + T^2$ because $\mathbf{x}_T = \mathbf{x}_0 + T\boldsymbol{\epsilon}$ for some Gaussian noise $\boldsymbol{\epsilon}$, $\sigma_{0T} = \sigma_0^2$, and $\text{SNR}_T/\text{SNR}_t = t^2/T^2$. One can show that the scaling functions then reduce to those in EDM. We leave details in Appendix A.5.

Generalized time-reversal. Due to the probability flow ODE's resemblance with classifier-guidance (Dhariwal and Nichol, 2021; Ho and Salimans, 2022), we can introduce an additional parameter w to set the "strength" of drift adjustment as below.

$$d\mathbf{x}_t = \Big[\mathbf{f}(\mathbf{x}_t, t) - g^2(t)\Big(\frac{1}{2}\mathbf{s}(\mathbf{x}_t, t, y, T) - w\mathbf{h}(\mathbf{x}_t, t, y, T)\Big)\Big]dt, \quad \mathbf{x}_T = y \tag{13}$$

which allows for a strictly wider class of marginal density of $\mathbf{x}_t$ generated by the resulting probability flow ODE. We examine the effect of this parameter in our ablation studies.

5 Stochastic Sampling for Denoising Diffusion Bridges

Although the probability flow ODE allows for one to use fast integration techniques to accelerate the sampling process (Zhang and Chen, 2022; Song et al., 2020a; Karras et al., 2022), purely

Algorithm 1 Denoising Diffusion Bridge Hybrid Sampler

Input: model $D_\theta(\mathbf{x}_t, t)$, time steps $\{t_i\}_{i=0}^N$, max time T, guidance strength w, step ratio s, distribution $q_{\text{data}}(\mathbf{y})$
Output: $\mathbf{x}_0$
Sample $\mathbf{x}_N \sim q_{\text{data}}(\mathbf{y})$
for $i = N, \dots, 1$ **do**
  Sample $\boldsymbol{\epsilon}_i \sim \mathcal{N}(\mathbf{0}, \boldsymbol{I})$
  $\hat{t}_i \leftarrow t_i + s(t_{i-1} - t_i)$
  $\boldsymbol{d}_i \leftarrow -\mathbf{f}(\mathbf{x}_i, t_i) + g^2(t_i)\Big(\mathbf{s}(\mathbf{x}_i, t_i, \mathbf{x}_N, T) - \mathbf{h}(\mathbf{x}_i, t_i, \mathbf{x}_N, T)\Big)$
  $\hat{\mathbf{x}}_i \leftarrow \mathbf{x}_i + \boldsymbol{d}_i(\hat{t}_i - t_i) + g(t_i)\sqrt{\hat{t}_i - t_i}\boldsymbol{\epsilon}_i$
  $\hat{\boldsymbol{d}}_i \leftarrow -\mathbf{f}(\hat{\mathbf{x}}_i, \hat{t}_i) + g^2(\hat{t}_i)\Big(\frac{1}{2}\mathbf{s}(\hat{\mathbf{x}}_i, \hat{t}_i, \mathbf{x}_N, T) - w\mathbf{h}(\hat{\mathbf{x}}_i, \hat{t}_i, \mathbf{x}_N, T)\Big)$
  $\mathbf{x}_{i-1} \leftarrow \hat{\mathbf{x}}_i + \hat{\boldsymbol{d}}_i(t_{i-1} - \hat{t}_i)$
  if $i \neq 1$ **then**
    $\boldsymbol{d}'_i \leftarrow -\mathbf{f}(\mathbf{x}_{i-1}, t_{i-1}) + g^2(t_{i-1})\Big(\frac{1}{2}\mathbf{s}(\mathbf{x}_{i-1}, t_{i-1}, \mathbf{x}_N, T) - w\mathbf{h}(\mathbf{x}_{i-1}, t_{i-1}, \mathbf{x}_N, T)\Big)$
    $\mathbf{x}_{i-1} \leftarrow \hat{\mathbf{x}}_i + (\frac{1}{2}\boldsymbol{d}'_i + \frac{1}{2}\hat{\boldsymbol{d}}_i)(t_{i-1} - \hat{t}_i)$
  end if
end for

following an ODE path is problematic because diffusion bridges have fixed starting points given as data $\mathbf{x}_T = \mathbf{y} \sim q_{\text{data}}(\mathbf{y})$, and following the probability flow ODE backward in time generates a deterministic "expected" path. This can result in "averaged" or blurry outputs given initial conditions. Thus, we are motivated to introduce noise into our sampling process to improve the sampling quality and diversity.

Higher-order hybrid sampler. Our sampler is built upon prior higher-order ODE sampler in (Karras et al., 2022), which discretizes the sampling steps into $t_N > t_{N-1} > \cdots > t_0$ with decreasing intervals (see Appendix A.6 for details). Inspired by the predictor-corrector sampler introduced by Song et al. (2020b), we additionally introduce a scheduled Euler-Maruyama step which follows the backward SDE in between higher-order ODE steps. This ensures that the marginal distribution at each step approximately stays the same. We introduce additional scaling hyperparameter s, which define a step ratio in between t_{i-1} and t_i such that the interval $[t_i - s(t_i - t_{i-1}), t_i]$ is used for Euler-Maruyama steps and $[t_{i-1}, t_i - s(t_i - t_{i-1})]$ is used for Heun steps, as described in Algorithm 1.

6 Related Works and Special Cases

Diffusion models. The advancements in diffusion models (Sohl-Dickstein et al., 2015; Ho et al., 2020; Song et al., 2020b) have improved state-of-the-art in image generation and outperformed GANs (Goodfellow et al., 2014). The success of diffusion models goes hand in hand with important design choices such as network design (Song et al., 2020b; Karras et al., 2022; Nichol and Dhariwal, 2021; Hoogeboom et al., 2023; Peebles and Xie, 2023), improved noise-schedules (Nichol and Dhariwal, 2021; Karras et al., 2022; Peebles and Xie, 2023), faster and more accurate samplers (Song et al., 2020a; Lu et al., 2022a;b; Zhang and Chen, 2022), and guidance methods (Dhariwal and Nichol, 2021; Ho and Salimans, 2022). Given the large body of literature on diffusion models for unconditional generation, which largely is based on these various design choices, we seek to design our bridge formulation to allow for a seamless integration with this literature. As such, we adopt a time-reversal perspective to directly extend these methods.

Diffusion bridges, Schödinger bridges, and Doob's h-transform. Diffusion bridges (Särkkä and Solin, 2019) are a common tool in probability theory and have been actively studied in recent years in the context of generative modeling (Liu et al., 2022b; Somnath et al., 2023; De Bortoli et al., 2021; Peluchetti; 2023). Heng et al. (2021) explores diffusion bridges conditioned on fixed starting/ending points and learns to simulate the time-reversal of the bridge given an approximation of the score $\nabla_{\mathbf{x}_t} \log p(\mathbf{x}_t)$. More recently, instead of considering bridges with fixed endpoints, Liu et al. (2022b) uses Doob's h-transform to bridge between arbitrary distributions. A forward bridge is learned via

score-matching by simulating entire paths during training. In contrast, other works (Somnath et al., 2023; Peluchetti), while also adopting Doob's h-transform, propose simulation-free algorithms for forward-time generation. Delbracio and Milanfar (2023) similarly constructs a Brownian Bridge for direct iteration and is successfully applied to image-restoration tasks. Another approach De Bortoli et al. (2021) proposes Iterative Proportional Fitting (IPF) to tractably solve Schödinger Bridge (SB) problems in translating between different distributions. Liu et al. (2023) is built on a tractable class of SB which results in a simulation-free algorithm and has demonstrated strong performance in image translation tasks. More recently, extending SB with IPF, Bridge-Matching (Shi et al., 2023) proposes to use Iterative Markovian Fitting to solve the SB problem. A similar algorithm is also developed by Peluchetti (2023) for distribution translation. A more related work to ours is Li et al. (2023), which proposes to directly reverse a Brownian Bridge for distribution translation in discrete time. Our method instead shows how to construct a bridge model from any existing VP and VE diffusion processes in continuous time, and Brownian Bridge (as considered in most previous works) is but a special case of VE bridges. We additionally show that, when implemented correctly, VP bridges can achieve very strong empirical performance. Although similar perspective can be derived using forward-time diffusion as in Peluchetti which also proposes VE/VP bridge schedules, our framework enjoys additional empirical (reusing diffusion designs) and theoretical (connection with OT-Flow-Matching(Lipman et al., 2023; Tong et al., 2023b) and Rectified Flow (Liu et al., 2022a)) benefits.

Flow and Optimal Transport Works based on Flow-Matching (Lipman et al., 2023; Tong et al., 2023b; Pooladian et al., 2023; Tong et al., 2023a) learn an ODE-based transport map to bridge two distributions. Lipman et al. (2023) has demonstrated that by matching the velocity field of predefined transport maps, one can create powerful generative models competitive with the diffusion counterparts. Improving this approach, Tong et al. (2023b); Pooladian et al. (2023) exploit potential couplings between distributions using minibatch simulation-free OT. Rectified Flow (Liu et al., 2022a) directly constructs the OT bridge and uses neural networks to fit the intermediate velocity field. Another line of work uses stochastic interpolants (Albergo and Vanden-Eijnden, 2023) to build flow models and directly avoid the use of Doob's h-functions and provide an easy way to construct interpolation maps between distributions. Albergo et al. (2023) presents a general theory with stochastic interpolants unifying flow and diffusion, and shows that a bridge can be constructed from both an ODE and SDE perspctive. Separate from these methods, our model uses a different denoising bridge score-matching loss than this class of models. Constructing from this perspective allows us to extend many existing successful designs of diffusion models (which are not directly applicable to these works) to the bridge framework and push state-of-the-art further for image translation while retaining strong performance for unconditional generation.

6.1 Special Cases of Denoising Diffusion Bridge Models

Case 1: Unconditional diffusion process (Song et al., 2020b). For unconditional diffusion processes (which map data to noise), we can first show that the marginal $p(\mathbf{x}_t)$ when $p(\mathbf{x}_0) = q_{\text{data}}(\mathbf{x})$ exactly matches that of a regular diffusion process when $\mathbf{x}_T \sim q_{\text{data}}(\mathbf{y} \mid \mathbf{x}) = \mathcal{N}(\alpha_T \mathbf{x}, \sigma_T^2 \boldsymbol{I})$. By taking expectation over $\mathbf{x}_T$ in Eq. (8), we have

$$p(\mathbf{x}_t \mid \mathbf{x}_0) = \mathcal{N}(\alpha_t \mathbf{x}_0, \sigma_t \boldsymbol{I}) \tag{14}$$

One can further show that during sampling, Eq. (6) and (7) reduce to the reverse SDE and ODE (respectively) of a diffusion process when $\mathbf{x}_T$ is sampled from a Gaussian. We leave derivation details to Appendix A.4.

Case 2: OT-Flow-Matching (Lipman et al., 2023; Tong et al., 2023b) and Rectified Flow (Liu et al., 2022a). These works learn to match deterministic dynamics defined through ODEs instead of SDEs. In this particular case, they work with "straight line" paths defined by $\mathbf{x}_T - \mathbf{x}_0$.

To see that our framework generalizes this, first let us define a family of diffusion bridges with variance scaled by $c \in (0, 1)$ such that $p(\mathbf{x}_t \mid \mathbf{x}_0, \mathbf{x}_T) = \mathcal{N}(\hat{\mu}_t, c^2 \hat{\sigma}_t^2 \boldsymbol{I})$ where $\hat{\mu}_t$ and $\hat{\sigma}_t$ are as defined in Eq. (8). One can therefore show that with a VE diffusion where $\sigma_t^2 = c^2 t$, given some fixed $\mathbf{x}_0$ and $\mathbf{x}_t$, *i.e.* $T = 1$, and $\mathbf{x}_t$ sampled from Eq. (8),

$$\lim_{c \to 0} \left[\mathbf{f}(\mathbf{x}_t, t) - c^2 g^2(t) \Big(\frac{1}{2} \nabla_{\mathbf{x}_t} \log p(\mathbf{x}_t \mid \mathbf{x}_0, \mathbf{x}_1) - \nabla_{\mathbf{x}_t} \log p(\mathbf{x}_1 \mid \mathbf{x}_t) \Big) \right] = \mathbf{x}_1 - \mathbf{x}_0 \tag{15}$$

Figure 3: Qualitative comparison with the most relevant baselines.

where inside the bracket is the drift of probability flow ODE in Eq. (7) given $\mathbf{x}_0$ and $\mathbf{x}_1$, and the right hand side is exactly the straight line path term. In other words, these methods learn to match the drift in the bridge probability flow ODE (with a specific VE schedule) in the noiseless limit. The score model can then be matched against $\mathbf{x}_T - \mathbf{x}_0$, with some additional caveat to handle additional input $\mathbf{x}_T$, our framework exactly reduces to that of OT-Flow-Matching and Rectified Flow (details in Appendix A.4).

7 Experiments

In this section we verify the generative capability of DDBM , and we want to answer the following questions: (1) How well does DDBM perform in image-to-image translation in pixel space? (2) Can DDBM perform well in unconditional generation when one side of the bridge reduces to Gaussian distribution? (3) How does the additional design choices introduced affect the final performance? Unless noted otherwise, we use the same VE diffusion schedule as in EDM for our bridge model by default. We leave further experiment details to Appendix B.

7.1 Image-to-Image Translation

We demonstrate that DDBM can deliver competitive results in general image-to-image translation tasks. We evaluate on datasets with different image resolutions to demonstrate its applicability on a variety of scales. We choose Edges→Handbags (Isola et al., 2017) scaled to 64×64 pixels, which contains image pairs for translating from edge maps to colored handbags, and DIODE-Outdoor (Vasiljevic et al., 2019) scaled to 256×256, which contains normal maps and RGB images of real-world outdoor scenes. For evaluation metrics, we use Fréchet Inception Distance (FID) (Heusel et al., 2017) and Inception Scores (IS) (Barratt and Sharma, 2018) evaluated on all training samples translation quality, and we use LPIPS (Zhang et al., 2018) and MSE (in $[-1, 1]$ scale) to measure perceptual similarity and translation faithfulness.

We compare with Pix2Pix (Isola et al., 2017), SDEdit (Meng et al., 2022), DDIB (Su et al., 2022), Rectified Flow (Liu et al., 2022a), and I^{2}SB (Liu et al., 2023) as they are built for image-to-image translation. For SDEdit we train unconditional EDM on the target domain, *e.g.* colored images, and initialize the translation by noising source image, *e.g.* sketches, and generate by EDM sampler given the noisy image. The other baseline methods are run with their respective repo while using the same network architecture as ours. Diffusion and transport-based methods are evaluated with the same number of function evaluations ($N = 40$, which is the default for EDM sampler for 64×64 images) to demonstrate our sampler's effectiveness in the regime when the number of sampling steps are low. Results are shown in Table 2 and additional settings are specified in Appendix B.

We observe that our model can perform translation with both high generation quality and faithfulness, and we find that VP bridges outperform VE bridges in some cases. In contrast, Rectified-Flow as an OT-based method struggles to perform well when the two domains share little low-level similarities (*e.g.* color, hue). DDIB also fails to produce coherent translation due to the wide differences in pixel-space distribution between the paired data. I^{2}SB comes closest to our method, but falls short when

	Edges→Handbags-64×64				DIODE-256×256			
	FID ↓	IS ↑	LPIPS ↓	MSE ↓	FID ↓	IS ↑	LPIPS ↓	MSE ↓
Pix2Pix (Isola et al., 2017)	74.8	4.24	0.356	0.209	82.4	4.22	0.556	0.133
DDIB (Su et al., 2022)	186.84	2.04	0.869	1.05	242.3	4.22	0.798	0.794
SDEdit (Meng et al., 2022)	26.5	**3.58**	0.271	0.510	31.14	5.70	0.714	0.534
Rectified Flow (Liu et al., 2022a)	25.3	2.80	0.241	0.088	77.18	5.87	0.534	0.157
I^2SB (Liu et al., 2023)	7.43	3.40	0.244	0.191	9.34	5.77	0.373	0.145
DDBM (VE)	2.93	3.58	**0.131**	**0.013**	8.51	6.03	**0.226**	**0.0107**
DDBM (VP)	**1.83**	**3.73**	0.142	0.0402	**4.43**	**6.21**	0.244	0.0839

Table 2: Quantitative evaluation of pixel-space image-to-image translation.

limited by computational constraints, *i.e.* NFE is low. We additionally show qualitative comparison with the most performant baselines in Figure 3. More visual results can be found in Appendix B.1.

7.2 Ablation Studies

We now study the effect of our preconditioning and hybrid samplers on generation quality in the context of both VE and VP bridge (see Appendix B for VP bridge parameterization). In the left column of Figure 4, we fix the guidance scale w at 1 and vary the Euler step size s from 0 to 0.9 to introduce stochasticity. We see a significant decrease in FID score as we increase s which produces the best performance at some value between 0 and 1 (*e.g.* $s = 0.3$ for Edges→Handbags). Figure 3 also shows that the ODE sampler (*i.e.* $s = 0$) produces blurry images while our hybrid sampler produces considerably sharper results. On the right column, we study the effect of w (from 0 to 1) with fixed s. We observe that VE bridges are not affected by the change in w whereas VP bridges heavily rely on setting $w = 1$. We hypothesize that this is due to the fact that VP bridges follow "curved paths" and destroy signals in between, so it is reliant on Doob's h-function for further guidance towards correct probability distribution.

We also study the effect of our preconditioning in Table 3. Our baseline without our preconditioning and our sampler is a simple model that directly matches output of the neural network to the training target and generates using EDM (Karras et al., 2022) sampler. We see that each introduced component further boosts the generation performance. Therefore, we can conclude that the introduced practical components are essential for the success of our DDBM .

(a) Edges→Handbags

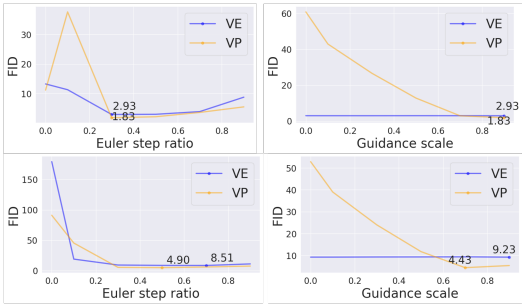

(b) DIODE

Figure 4: Ablation studies on Euler step ratio s and guidance scale w: $w = 1$ for all ablation on s and s is set to the best-performing value for each dataset for ablation on w.

Our precond.	Our sampler	E→H-64×64		DIODE-256×256	
		VE	VP	VE	VP
✗	✗	14.02	11.76	126.3	96.93
✓	✗	13.26	11.19	79.25	91.07
✗	✓	13.11	29.91	91.31	21.92
✓	✓	**2.93**	**1.83**	**8.51**	**4.43**

Table 3: Ablation study on the effect of sampler and preconditioning on FID. Cross mark on our preconditioning means no output reparameterization and directly use network output to match training target. Cross mark on our sampler means we reuse the ODE sampler from EDM with the same setting. E→H is a short-hand for Edges→Handbags.

7.3 Unconditional Generation

When one side of the distribution becomes Gaussian distribution, our framework exactly reduces to that of diffusion models. Specifically, during training when the end point $\mathbf{x}_T \sim \mathcal{N}(\alpha_T \mathbf{x}_0, \sigma_T^2 \boldsymbol{I})$,

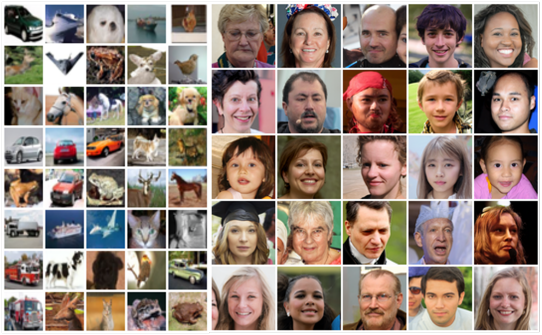

Figure 5: Generation on CIFAR-10 and FFHQ-64×64.

	CIFAR-10		FFHQ-64×64	
	NFE ↓	FID ↓	NFE ↓	FID ↓
DDPM [13]	1000	3.17	1000	3.52
DDIM [44]	50	4.67	50	5.18
DDPM++ [46]	1000	3.01	1000	3.39
NCSN++ [46]	1000	3.77	1000	25.95
Rectified Flow [24]	127	2.58	152	4.45
EDM [18]	35	**2.04**	79	2.53
DDBM	35	2.06	79	**2.44**

Table 4: Evaluation of unconditional generation.

our intermediate bridge samples $\mathbf{x}_t$ follows the distribution $\mathbf{x}_t \sim \mathcal{N}(\alpha_t \mathbf{x}_0, \sigma_t^2 \boldsymbol{I})$. We empirically verify that using our bridge sampling and the pred-$\mathbf{x}$ objective inspired by EDM, we can recover its performance by using our more generalized parameterization.

We evaluate our method on CIFAR-10 (Krizhevsky et al., 2009) and FFHQ-64×64 (Karras et al., 2019) which are processed according to Karras et al. (2022). We use FID score for quantitative evaluation using 50K generated images and use number of function evaluations (NFE) for generation efficiency. We compare our generation results against diffusion-based and optimal transport-based models including DDPM (Ho et al., 2020), DDIM (Song et al., 2020a), DDPM++ (Song et al., 2020b), NCSN++ (Song et al., 2020b), Rectified Flow (Liu et al., 2022a), EDM (Karras et al., 2022). Quantitative results are presented in Table 4 and generated samples are shown in Figure 5.

We observe that our model is able to match EDM performance with negligible degradation in FID scores for CIFAR-10 and marginal improvement for FFHQ-64×64. This corroborates our claim that our method can benefit from advances in diffusion models and generalize many of the advanced parameterization techniques such as those introduced in EDM.

8 Conclusion

In this work, we introduce Denoising Diffusion Bridge Models, a novel class of models that builds a stochastic bridge between paired samples with tractable marginal distributions in between. The model is learned by matching the conditional score of a tractable bridge distribution, which allows one to transport from one distribution to another via a new reverse SDE or probability flow ODE. Additionally, this generalized framework shares many similarities with diffusion models, thus allowing us to reuse and generalize many designs of diffusion models. We believe that DDBM is a significant contribution towards a general framework for distribution translation. In the era of generative AI, DDBM has a further role to play.

REFERENCES

Michael S Albergo, Nicholas M Boffi, and Eric Vanden-Eijnden. Stochastic interpolants: A unifying framework for flows and diffusions. *arXiv preprint arXiv:2303.08797*, 2023.

Michael Samuel Albergo and Eric Vanden-Eijnden. Building normalizing flows with stochastic interpolants. In *The Eleventh International Conference on Learning Representations*, 2023. URL `https://openreview.net/forum?id=li7qeBbCR1t`.

Shane Barratt and Rishi Sharma. A note on the inception score. *arXiv preprint arXiv:1801.01973*, 2018.

Valentin De Bortoli, James Thornton, Jeremy Heng, and Arnaud Doucet. Diffusion schrödinger bridge with applications to score-based generative modeling. *Advances in Neural Information Processing Systems*, 34: 17695–17709, 2021.

Mauricio Delbracio and Peyman Milanfar. Inversion by direct iteration: An alternative to denoising diffusion for image restoration. *arXiv preprint arXiv:2303.11435*, 2023.

Bernard Delyon and Ying Hu. Simulation of conditioned diffusion and application to parameter estimation. *Stochastic Processes and their Applications*, 116(11):1660–1675, 2006.

Prafulla Dhariwal and Alexander Nichol. Diffusion models beat gans on image synthesis. *Advances in Neural Information Processing Systems*, 34:8780–8794, 2021.

Joseph L Doob and JI Doob. *Classical potential theory and its probabilistic counterpart*, volume 262. Springer, 1984.

Ian J. Goodfellow, Jean Pouget-Abadie, Mehdi Mirza, Bing Xu, David Warde-Farley, Sherjil Ozair, Aaron C. Courville, and Yoshua Bengio. Generative adversarial nets. In *NIPS*, 2014.

Jeremy Heng, Valentin De Bortoli, Arnaud Doucet, and James Thornton. Simulating diffusion bridges with score matching. *arXiv preprint arXiv:2111.07243*, 2021.

Martin Heusel, Hubert Ramsauer, Thomas Unterthiner, Bernhard Nessler, and Sepp Hochreiter. Gans trained by a two time-scale update rule converge to a local nash equilibrium. *Advances in neural information processing systems*, 30, 2017.

Jonathan Ho and Tim Salimans. Classifier-free diffusion guidance. *arXiv preprint arXiv:2207.12598*, 2022.

Jonathan Ho, Ajay Jain, and Pieter Abbeel. Denoising diffusion probabilistic models. *Advances in Neural Information Processing Systems*, 33:6840–6851, 2020.

Jonathan Ho, William Chan, Chitwan Saharia, Jay Whang, Ruiqi Gao, Alexey Gritsenko, Diederik P Kingma, Ben Poole, Mohammad Norouzi, David J Fleet, et al. Imagen video: High definition video generation with diffusion models. *arXiv preprint arXiv:2210.02303*, 2022.

Emiel Hoogeboom, Jonathan Heek, and Tim Salimans. simple diffusion: End-to-end diffusion for high resolution images. *arXiv preprint arXiv:2301.11093*, 2023.

Phillip Isola, Jun-Yan Zhu, Tinghui Zhou, and Alexei A Efros. Image-to-image translation with conditional adversarial networks. In *Proceedings of the IEEE conference on computer vision and pattern recognition*, pages 1125–1134, 2017.

Tero Karras, Samuli Laine, and Timo Aila. A style-based generator architecture for generative adversarial networks. In *Proceedings of the IEEE/CVF conference on computer vision and pattern recognition*, pages 4401–4410, 2019.

Tero Karras, Miika Aittala, Timo Aila, and Samuli Laine. Elucidating the design space of diffusion-based generative models. *arXiv preprint arXiv:2206.00364*, 2022.

Diederik Kingma, Tim Salimans, Ben Poole, and Jonathan Ho. Variational diffusion models. *Advances in neural information processing systems*, 34:21696–21707, 2021.

Alex Krizhevsky, Geoffrey Hinton, et al. Learning multiple layers of features from tiny images. 2009.

Bo Li, Kaitao Xue, Bin Liu, and Yu-Kun Lai. Bbdm: Image-to-image translation with brownian bridge diffusion models. In *Proceedings of the IEEE/CVF Conference on Computer Vision and Pattern Recognition*, pages 1952–1961, 2023.

Yaron Lipman, Ricky T. Q. Chen, Heli Ben-Hamu, Maximilian Nickel, and Matthew Le. Flow matching for generative modeling. In *The Eleventh International Conference on Learning Representations*, 2023. URL https://openreview.net/forum?id=PqvMRDCJT9t.

Guan-Horng Liu, Arash Vahdat, De-An Huang, Evangelos A Theodorou, Weili Nie, and Anima Anandkumar. I^2sb: Image-to-image schrödinger bridge. *arXiv*, 2023.

Xingchao Liu, Chengyue Gong, and Qiang Liu. Flow straight and fast: Learning to generate and transfer data with rectified flow. *arXiv preprint arXiv:2209.03003*, 2022a.

Xingchao Liu, Lemeng Wu, Mao Ye, and Qiang Liu. Let us build bridges: Understanding and extending diffusion generative models. *arXiv preprint arXiv:2208.14699*, 2022b.

Cheng Lu, Yuhao Zhou, Fan Bao, Jianfei Chen, Chongxuan Li, and Jun Zhu. Dpm-solver: A fast ode solver for diffusion probabilistic model sampling in around 10 steps. *arXiv preprint arXiv:2206.00927*, 2022a.

Cheng Lu, Yuhao Zhou, Fan Bao, Jianfei Chen, Chongxuan Li, and Jun Zhu. Dpm-solver++: Fast solver for guided sampling of diffusion probabilistic models. *arXiv preprint arXiv:2211.01095*, 2022b.

Chenlin Meng, Yutong He, Yang Song, Jiaming Song, Jiajun Wu, Jun-Yan Zhu, and Stefano Ermon. SDEdit: Guided image synthesis and editing with stochastic differential equations. In *International Conference on Learning Representations*, 2022.

Alexander Quinn Nichol and Prafulla Dhariwal. Improved denoising diffusion probabilistic models. In *International Conference on Machine Learning*, pages 8162–8171. PMLR, 2021.

William Peebles and Saining Xie. Scalable diffusion models with transformers. In *Proceedings of the IEEE/CVF International Conference on Computer Vision*, pages 4195–4205, 2023.

Stefano Peluchetti. Non-denoising forward-time diffusions.

Stefano Peluchetti. Diffusion bridge mixture transports, schr\" odinger bridge problems and generative modeling. *arXiv preprint arXiv:2304.00917*, 2023.

Aram-Alexandre Pooladian, Heli Ben-Hamu, Carles Domingo-Enrich, Brandon Amos, Yaron Lipman, and Ricky Chen. Multisample flow matching: Straightening flows with minibatch couplings. *arXiv preprint arXiv:2304.14772*, 2023.

Aditya Ramesh, Prafulla Dhariwal, Alex Nichol, Casey Chu, and Mark Chen. Hierarchical text-conditional image generation with clip latents. *ArXiv*, abs/2204.06125, 2022.

L Chris G Rogers and David Williams. *Diffusions, Markov processes and martingales: Volume 2, Itô calculus*, volume 2. Cambridge university press, 2000.

Robin Rombach, Andreas Blattmann, Dominik Lorenz, Patrick Esser, and Björn Ommer. High-resolution image synthesis with latent diffusion models. In *Proceedings of the IEEE/CVF Conference on Computer Vision and Pattern Recognition*, pages 10684–10695, 2022.

Chitwan Saharia, William Chan, Huiwen Chang, Chris A. Lee, Jonathan Ho, Tim Salimans, David J. Fleet, and Mohammad Norouzi. Palette: Image-to-image diffusion models. *ACM SIGGRAPH 2022 Conference Proceedings*, 2021.

Tim Salimans and Jonathan Ho. Progressive distillation for fast sampling of diffusion models. *arXiv preprint arXiv:2202.00512*, 2022.

Simo Särkkä and Arno Solin. *Applied stochastic differential equations*, volume 10. Cambridge University Press, 2019.

Moritz Schauer, Frank Van Der Meulen, and Harry Van Zanten. Guided proposals for simulating multi-dimensional diffusion bridges. 2017.

Yuyang Shi, Valentin De Bortoli, Andrew Campbell, and Arnaud Doucet. Diffusion schr\" odinger bridge matching. *arXiv preprint arXiv:2303.16852*, 2023.

Jascha Sohl-Dickstein, Eric Weiss, Niru Maheswaranathan, and Surya Ganguli. Deep unsupervised learning using nonequilibrium thermodynamics. In *International Conference on Machine Learning*, pages 2256–2265. PMLR, 2015.

Vignesh Ram Somnath, Matteo Pariset, Ya-Ping Hsieh, Maria Rodriguez Martinez, Andreas Krause, and Charlotte Bunne. Aligned diffusion schr\" odinger bridges. *arXiv preprint arXiv:2302.11419*, 2023.

Jiaming Song, Chenlin Meng, and Stefano Ermon. Denoising diffusion implicit models. *arXiv preprint arXiv:2010.02502*, 2020a.

Yang Song and Stefano Ermon. Generative modeling by estimating gradients of the data distribution. *Advances in neural information processing systems*, 32, 2019.

Yang Song, Jascha Sohl-Dickstein, Diederik P Kingma, Abhishek Kumar, Stefano Ermon, and Ben Poole. Score-based generative modeling through stochastic differential equations. *arXiv preprint arXiv:2011.13456*, 2020b.

Xuan Su, Jiaming Song, Chenlin Meng, and Stefano Ermon. Dual diffusion implicit bridges for image-to-image translation. In *The Eleventh International Conference on Learning Representations*, 2022.

Juraj Szavits-Nossan and Martin R Evans. Inequivalence of nonequilibrium path ensembles: the example of stochastic bridges. *Journal of Statistical Mechanics: Theory and Experiment*, 2015(12):P12008, 2015.

Alexander Tong, Nikolay Malkin, Kilian Fatras, Lazar Atanackovic, Yanlei Zhang, Guillaume Huguet, Guy Wolf, and Yoshua Bengio. Simulation-free schr\" odinger bridges via score and flow matching. *arXiv preprint arXiv:2307.03672*, 2023a.

Alexander Tong, Nikolay Malkin, Guillaume Huguet, Yanlei Zhang, Jarrid Rector-Brooks, Kilian Fatras, Guy Wolf, and Yoshua Bengio. Improving and generalizing flow-based generative models with minibatch optimal transport. In *ICML Workshop on New Frontiers in Learning, Control, and Dynamical Systems*, 2023b.

Igor Vasiljevic, Nick Kolkin, Shanyi Zhang, Ruotian Luo, Haochen Wang, Falcon Z. Dai, Andrea F. Daniele, Mohammadreza Mostajabi, Steven Basart, Matthew R. Walter, and Gregory Shakhnarovich. DIODE: A Dense Indoor and Outdoor DEpth Dataset. *CoRR*, abs/1908.00463, 2019. URL `http://arxiv.org/abs/1908.00463`.

Cédric Villani. Optimal transport: Old and new. 2008.

Qinsheng Zhang and Yongxin Chen. Fast sampling of diffusion models with exponential integrator. *arXiv preprint arXiv:2204.13902*, 2022.

Richard Zhang, Phillip Isola, Alexei A Efros, Eli Shechtman, and Oliver Wang. The unreasonable effectiveness of deep features as a perceptual metric. In *CVPR*, 2018.

Jun-Yan Zhu, Taesung Park, Phillip Isola, and Alexei A. Efros. Unpaired image-to-image translation using cycle-consistent adversarial networks. *2017 IEEE International Conference on Computer Vision (ICCV)*, pages 2242–2251, 2017.